Ideal kink mode benchmark

J. R. Myra, D. A. Baver

Lodestar Research Corp., 2400 Central Ave. P-5, Boulder, Colorado 80301

M. V. Umansky

Lawrence Livermore National Laboratory, Livermore, CA 94550

A. Introduction

This test was devised to verify the ability of the 2DX eigenvalue code to correctly solve a fluid model relevant to Edge Localized Mode (ELM) physics in tokamaks, viz. the current-driven ideal kink mode. Kink/peeling mode instability physics, in combination with pressure gradient-driven instability physics is believed to be responsible for Type I ELM onset.[1] Since the functionality of the 2DX code depends on both the source code itself and the input file defining the system of equations to solve (structure file), this test demonstrates both. Similar tests have been performed using other physics models. Moreover, since the structure file for these tests represents a subset of a more general 6-field model, many of the terms in that test are also verified. A more detailed description of the 2DX code can be found in Ref. 2.

The present test compares 2DX results to asymptotic analytic results based on a sharp boundary solution[3] of the eigenvalue problem, with some additional analytic embellishments to Ref. 3 described here. In particular, a strict sharp boundary limit is unsuitable as a benchmark test case because it cannot be resolved numerically with a finite grid. Thus, we extend the analytical result to account for small departures from the strict sharp boundary limit.

B. Ideal kink mode model

To benchmark the current gradient drive term in the ideal MHD model, we solve the equation

$$\gamma^2\left(\nabla_\perp^2\delta\Phi\right)=\mu\delta_{er}^2\frac{B^2}{n}\partial_\parallel\nabla_\perp^2\nabla_\parallel\delta\Phi-\frac{ik_b B(\partial_r J_\parallel)}{n}\nabla_\parallel\delta\Phi \qquad (1)$$

This equation may be obtained from the primitive six-field eigenvalue equations (see e.g. Ref. 2) by combining the equations for vorticity and Ohm-Ampere's law in the ideal MHD limit. Here, we work in Bohm-normalized variables with times normalized to $1/\Omega_i$, lengths normalized to a reference sound gyroradius ρ_{sr}, temperature and electrostatic potential Φ/e to a reference value of electron temperature T_{er}, and density to a reference value of density n_{er} In Eq. (1), $\mu = m_i/m_e$, $\delta_{er}^2 = c^2/(\rho_{sr}^2\omega_{pe}^2)$ and for any Q,

$\partial_{\|} Q = B\nabla_{\|} (B^{-1}Q)$, $\partial_r = RB_p \partial/\partial\psi$, k_b is the binormal component of the perpendicular wavenumber; other symbols have their usual meanings.

For the benchmark test set we take B = n = 1, and since there is no variation in the equilibrium along B, for analytical work $\nabla_{\|} = ik_{\|}$ (in the code, parallel variation is solved for numerically).

$$\left(\gamma^2 + \mu\delta_{er}^2 k_{\|}^2\right)\left(\nabla_{\perp}^2 \delta\Phi\right) = k_b k_{\|} (\partial_r J_{\|})\delta\Phi \tag{2}$$

The current profile is taken as a sharply varying step function in the next section, while corrections for smoothed profiles are given in the Appendix. The analytical solution and benchmark test is carried out in the cylindrical tokamak model.

B. Analytical solution

For a strict sharp boundary $J_{\|}$ profile, ($J_{\|} = J_{\|0}$ to the left, and 0 to the right) with step at r = a, we solve the equation

$$\nabla_{\perp}^2 \delta\Phi = (\partial_r^2 - k_b^2)\delta\Phi = 0 \tag{3}$$

in each region to obtain

$$\delta\Phi = \exp(\pm k_b (r - a)) \tag{4}$$

Then integrate Eq. (2) across the step to get the jump condition

$$\left(\gamma^2 + \mu\delta_{er}^2 k_{\|}^2\right)\left(\partial_r \delta\Phi\right)\Big|_{r=a} = -k_b k_{\|} J_{\|0}\delta\Phi \tag{5}$$

where $[J_{\|}] = -J_{\|0}$. The dispersion relation is obtained by employing Eq. (4) in Eq. (5)

$$\gamma^2 + \mu\delta_{er}^2 k_{\|}^2 - k_{\|} J_{\|0}/2 = 0 \tag{6}$$

In dimensional units

$$\omega^2 - k_{\|}^2 v_a^2 + k_{\|}\frac{J_{\|0}}{2} = 0 \tag{7}$$

where v_a is the Alfvén velocity. For the sharp boundary equilibrium model (making $J_{\|}$ consistent with q)

$$J_{\|0} = \frac{2v_a^2}{qR} \rightarrow \frac{2\mu\delta_{er}^2\rho_s}{qR} \tag{8}$$

$$\hat{\omega}^2 - \hat{k}_{\|}^2 + \hat{k}_{\|} = 0 \tag{9}$$

where $\hat{\omega} = \omega qR/v_a$, $\hat{k}_{\|} = k_{\|} qR$. Maximum growth is at $\hat{k}_{\|} = 1/2$ and is $\hat{\omega} = i/2$. This implies

$$\gamma_{max} = \frac{\mu^{1/2}\delta_{er}}{2qR} \quad \text{(Bohm dimensionless)}$$

This result is similar to that obtained in Ref. 3, but the inertial term is twice as large here because we have assumed a constant density profile (rather than taking it as a step function also.)

The above can be generalized to include a finite wall position, and to correct for a sharp but finite-width tanh function instead of a strict step function. The generalized dispersion relation takes the form

$$\hat{\omega}^2 - \hat{k}_{||}^2 + W\hat{k}_{||} = 0 \tag{10}$$

where W is derived in the Appendix.

C. Numerical solution and comparison

We solve Eq. (1) with 2DX on a $n_x \times n_y = 511\times128$ grid. Dimensionless input parameters are $\mu = 3672$, $\delta_{er}^2 = 0.08449$, $1/(qR) = 1.8758\times10^{-4}$ and the reference values employed for dimensional results are $\Omega_i = 9.58\times10^7$/s, $\omega_a = v_a/(qR) = 3.1657\times10^5$/s. The current profile is taken as

$$J_{||} = \frac{J_{||0}}{2}\left(1 - \tanh\left(\frac{r-a}{z_w}\right)\right) \tag{11}$$

where $z_w = 0.002$ and $J_{||0}$ is given by Eq. (8).

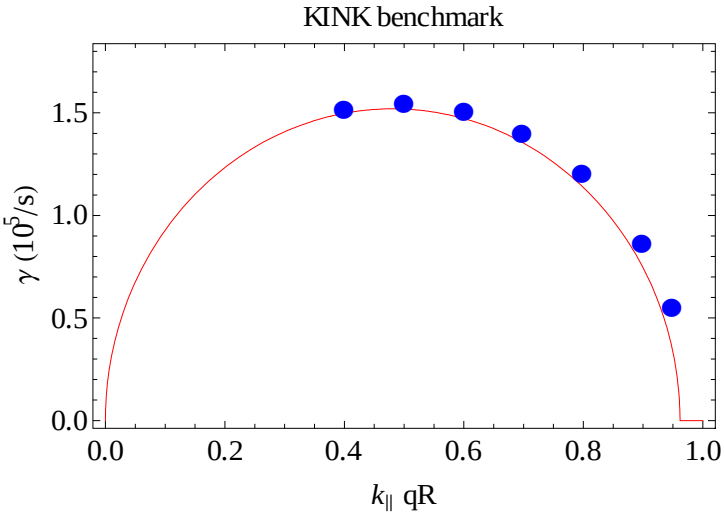

Fig. 1 Growth rate $\gamma(10^5/s)$ vs. normalized $k_{||}$ for 2DX (blue dots) and for the solution of Eq. (10) retaining finite step width corrections for the current gradient. Finite wall position corrections are negligible.

Because of the high resolution, these runs take several hours each, although the resolution of the rather sharp current gradient is still not superb. For these runs, W = 0.962 from the finite width corrections, while the finite wall positions are negligible (hence the value of k_b or toroidal mode number n = 20 that was employed drops out.) Results are shown in Fig. 1.

In Fig. 1, cases with $k_{||}qR < 0.5$ are awkward numerically since the fundamental parallel mode in the box is not usually the fastest growing mode. In these cases 2DX will report the fastest mode to be a poorly resolved harmonic. The desired mode can be found by picking through the spectrum, but this has not been done except for the case with $k_{||}qR < 0.4$. There is no reason to suspect problems in benchmarking these cases, it is just inconvenient.

Appendix: Corrections for finite wall position and finite width step

For conducting wall BCs, ($\delta\Phi = 0$) at finite locations on each side of the step, $z = \pm z_w$, where $z = r - a$ is a shifted radial variable centered at the step, we can modify Eqs. (3) and (4) as follows

$$\delta\Phi = \exp(-k_b z) \rightarrow \frac{\sinh(k_b(z_w - z))}{\sinh(k_b z_w)} \tag{A1}$$

$$\partial_r \delta\Phi\big|_{r=a} = -k_b \rightarrow -k_b \coth k_b z_w \tag{A2}$$

So in the dispersion relation, Eq. (7), after dividing through, the drive term $J_{||0}$ is multiplied by $\tanh(k_b z_w)$. Similarly, one can derive the correction for insulating BCs, $\partial_r \delta\Phi(z_w) = 0$. In summary we find

$$W = \begin{cases} \tanh(k_b z_w), & \text{conducting BCs} \\ \coth(k_b z_w), & \text{insulating BCs} \end{cases} \tag{A3}$$

We can also derive corrections for a finite current profile width. The idea is to do a perturbative expansion in the width z_m where the current profile is given by

$$J(z) = \frac{J_{||0}}{2}\left(1 - \tanh(z/z_m)\right) \tag{A4}$$

In leading order, we take the solution to be that of the step-function model (for simplicity, the infinite wall case), given by Eq. (4). Then in the vicinity of z_m for $k_b z_m << 1$ we can take $\delta\Phi = 1$ and an equation accurate through next order is

$$\gamma_a^2(\partial_z^2 - k_b^2)\delta\Phi = k_b k_{||}(\partial_r J_{||}) \tag{A5}$$

where

$$\gamma_a^2 \equiv \gamma^2 + \mu\delta_{er}^2 k_{||}^2 \tag{A6}$$

Integrating from z = 0 (noting even parity of $\delta\Phi$), and dropping $k_b z_m$ contributions gives

$$\partial_z \delta\Phi = \frac{k_b k_{||}}{\gamma_a^2}(J_{||} - J_{||0}/2) \tag{A7}$$

$$\delta\Phi = 1 + \frac{k_b k_{||}}{\gamma_a^2}\int_0^z dz\, J_{||} - \frac{k_b k_{||}}{2\gamma_a^2} J_{||0} z \tag{A8}$$

Next we match the logarithmic derivatives at a point z_1 such that

$$z_m << z_1 << 1/k_b \tag{A9}$$

i.e. z_1 is outside the current profile gradient, but inside the region where $k_b z_m << 1$ holds. The matching condition is

$$\left(\frac{\partial_z \delta\Phi}{\delta\Phi}\right)_{z_1} = -k_b \tag{A10}$$

$$\frac{-\dfrac{k_b k_{||} J_{||0}}{2\gamma_a^2}}{1 + \dfrac{k_b k_{||}}{\gamma_a^2}\displaystyle\int_0^{z_1} dz\, J_{||} - \dfrac{k_b k_{||}}{2\gamma_a^2} J_{||0} z_1} = -k_b \tag{A11}$$

After cleaning up, this reduces to

$$\gamma^2 + \mu\delta_{er}^2 k_{||}^2 - \frac{k_{||} J_{||0}}{2}\left(1 - 2k_b \int_0^{z_1} dz\, \frac{J_{||}}{J_{||0}}\right) = 0 \tag{A12}$$

where the $J_{||0} z_1$ term in Eq. (11) was dropped since it is small in $k_b z_1$ relative to the other $J_{||0}$ term. This correction enters in the form shown in Eq. (10) and gives

$$W = 1 - 2k_b \int_0^{\infty} dz \frac{1}{2}\left(1 - \tanh(z/z_m)\right) \tag{A13}$$

or

$$W = 1 - k_b z_m \ln 2 \tag{A14}$$

If both finite wall and finite width corrections need to be applied, and they are both small corrections, the W's can be multiplied together.

References

1. P. B. Snyder, H. R. Wilson, and X. Q. Xu, Phys. Plasmas **12**, 056115 (2005).
2. D. A. Baver, J. R. Myra and M.V. Umansky, Comp. Phys. Comm. **182**, 1610, (2011).
3. D. A. D'Ippolito, J. R. Myra, S.C. Jardin, M.S. Chance and E.J. Valeo, Phys. of Plasmas **2**, 3429 (1995); and refs therein.